Progress In Electromagnetics Research C, Vol. 23, 83–93, 2011

DUAL-MODE CPW-FED DOUBLE SQUARE-LOOP RESONATORS FOR WLAN AND WIMAX TRI-BAND DESIGN

C. Y. Liu[1], B. H. Zeng[2], J. C. Liu[2,*], C. C. Chen[3], and D. C. Chang[4]

[1]Department of Electronics Engineering, Tahwa Institute of Technology, Qionglin, Hsinchu 307, Taiwan, R.O.C.

[2]Department of Electrical Engineering, Ching Yun University, Chung-Li, Tao-Yuan 32097, Taiwan, R.O.C.

[3]Department of Electrical Engineering, Feng Chia University, Taichung 407, Taiwan, R.O.C.

[4]Department of Communication Engineering, Oriental Institute of Technology, Pan-Chiao Area, New Taipei 22061, Taiwan, R.O.C.

Abstract—An improved CPW-fed configurations with dual-mode double-square-ring resonators (DMDSRR) for tri-band application is proposed in this paper. The resonant frequency equations related to DMDSRR geometry are introduced for simply designing tri-band bandpass filter (BPF). Resonant frequencies and transmission zeroes can be controlled by tuning the perimeter ratio of the square rings. To obtain lower insertion loss, higher out-of-band rejection level and wider bandwidth of tri-band, the improved coplanar waveguide (CPW) fed and the step impedance resonator (SIR) and meander line dual-mode perturbations are designed. The effective design procedure is provided. The proposed filter is successfully simulated and measured. It can be applied to WLAN (2.45, 5.20 and 5.80 GHz) and WiMAX (3.50 GHz) systems.

Received 3 July 2011, Accepted 27 July 2011, Scheduled 3 August 2011

* Corresponding author: Ji-Chyun Liu (jichyun@cyu.edu.tw).

1. INTRODUCTION

The increasing demand for multi-band applications has required a single wireless transceiver to support multi-band operations. The multi-band BPFs play an important role in a multi-band transceiver, such as dual-band [1–4], tri-band [5–19] and quad-band [20–22] filters.

Recently, a new excitation for DMDSRR with CPW was proposed for dual-band applications [1]. The square ring resonators with back-to-back and concentric configurations were presented. Due to the effect of the CPW input/output structure, performance with low insertion loss and high out-of-band rejection level was achieved. In [5], the even/odd-mode method with equivalent circuit was proposed and designed with the split-ring resonator (SRR) to obtain three controllable resonant frequencies. In [6], the coupling-matrix design for tri-band filter was presented. In [7], the authors developed the frequency transformation for finding the locations of poles and zeros of specific tri-band filters. Moreover, various filters have been realized with the basic SIR and their variety to exhibit tri-band responses [8–13, 15]. Recently, for tri-band filter design, the stub-loaded resonators (SLR) and half-wavelength resonators were presented [16]. And a microstrip and a defeated ground structure (DGS) slot were used [17]. Applied for WLAN and WiMAX tri-band systems, the open and short stubs loaded crossed resonator were designed [14]. And the SLR and DGS resonator were used [18].

Whether the combined quarter-wavelength SIR or assembled half-wavelength SIR was used, the impedance ratio computation and tuning the stub were needed [9–12, 19]. For SLR filter, the stub length was tuned for the desired responses [12, 16–18]. On the other hand, in [8], three closed-form equations related to the resonant frequencies of the tri-band were deduced for simple design. Similarly, in [21], four simple equations related to the perimeters of the concentric rings were approximated for the quad-band design.

Based on [1] and [21], this paper proposes a novel way with the resonant frequency equations related to DMDSRR geometry for simply designing tri-band BPF. It can be applied to WLAN (2.45, 5.20 and 5.80 GHz) and WiMAX (3.50 GHz) tri-band systems. Tuning the perimeter ratios of the rings presents the controllable resonant frequencies. For excitation of DMDSRR, the filter is fed by an improved CPW-fed line. The improved CPW-fed line consists of a twin-T feed line and the branches with slits. In addition, by using novel SIR and square perturbations, the novel dual-mode DMDSRR is proposed. The simulation and measurement results, including frequency responses and tri-band versus perimeter ratio, are presented to analyze the tri-band characteristic.

2. FILTER CONFIGURATIONS AND BASIS

The perimeters of the square rings are related to the guided wavelength at corresponding resonant frequencies. Thus, the resonant frequencies of the tri-band can be approximately expressed as [21, 23]:

$$f_1 = \frac{c}{4L_1\sqrt{\varepsilon_{eff}}} \tag{1}$$

$$f_2 = \frac{c}{(4L_2+\Delta\ell)\sqrt{\varepsilon_{eff}}} \tag{2}$$

$$f_{3a} = \frac{c}{2L_1\sqrt{\varepsilon_{eff}}} \tag{3}$$

$$f_{3b} = \frac{c}{(2L_2+\Delta\ell)\sqrt{\varepsilon_{eff}}} \tag{4}$$

$$\Delta\ell = W_3 + W_4 - g_1 \tag{5}$$

where c is the speed of light in free space, L_1 and L_2 denote the side lengths of the two rings, and ε_{eff} represents the effective permittivity of the substrates.

The ring related to the larger side-length (L_1) decides the resonant frequencies f_1 in first band and the f_{3a} in third band, and the ring related to the smaller side-length (L_2) represents the resonant frequencies f_2 in second band and the f_{3b} in third band shown in Fig. 1(a). The electrical length of $\Delta\ell$ related to the meander line is used to increase the perimeter of the smaller ring. Both f_{3a} and f_{3b} are the lower and upper resonant frequencies in the third band. The ring perimeters will be utilized to control the center frequencies. It can be obtained from (1), (2), (3) and (4) as follows:

$$\frac{L_2}{L_1} = \frac{f_1}{f_2} = \frac{f_{3a}}{f_{3b}} \tag{6}$$

Based on (6), two perimeters can be properly selected to facilitate the filter design.

Obviously, it is difficult to feed the square rings if the length difference of the two side lengths is quite large. Therefore, the CPW with parallel couplings is preferred. For dual-band responses, the square rings were fed by a twin-T CPW [1]. For excitation of tri-band responses, the square rings are fed by an improved twin-T CPW. The improved twin-T CPW consists of a feed-line and the branches with the slits shown in Fig. 1(b). The widths of the slits are expressed by W_{g1}, and the length is L_{g1}. Transmission zeros can be obtained

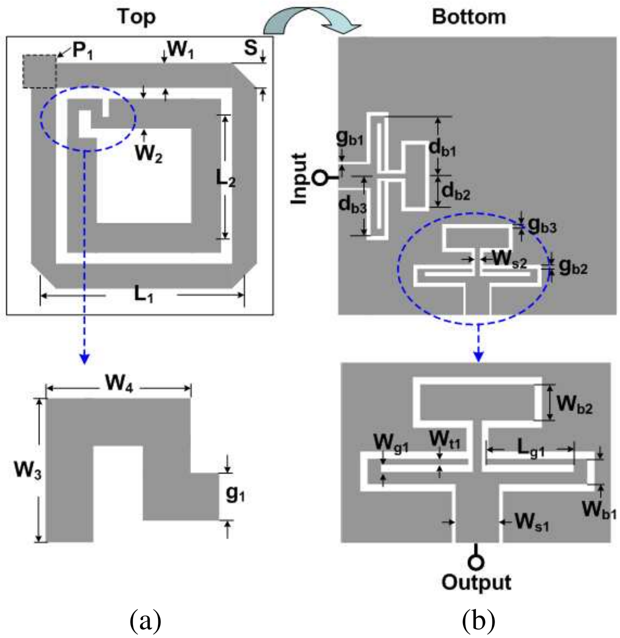

Figure 1. CPW-fed DMDSLR configurations. (a) Top view DMDSLR. (b) Bottom view twin-T CPW.

by tuning W_{g1}, and L_{g1}. The width of $50\,\Omega$ line is given by W_{s1}, and the spacing is given by g_{b1}. Impedance matching can be improved by adjusting W_{s1} and g_{b1}.

Physical dimensions are stated:

(a) Tri-band DMDSLR with $L_1 = 20.2\,\text{mm}$, $L_2 = 12.5\,\text{mm}$, $S = 3.54\,\text{mm}$, $W_1 = 2.5\,\text{mm}$, $W_2 = 3.0\,\text{mm}$, $W_3 = 3.5\,\text{mm}$, $W_4 = 3.55\,\text{mm}$, $P_1 = 3.3 \times 3.3\,\text{mm}^2$, and $g_1 = 1.17\,\text{mm}$.

(b) twin-T CPW_1 configuration with $d_{b1} = d_{b3} = 6.045\,\text{mm}$, $d_{b2} = 3.15\,\text{mm}$, $g_{b1} = 0.2\,\text{mm}$, $g_{b2} = 0.4\,\text{mm}$, $g_{b3} = 0.4\,\text{mm}$, $W_{s1} = 2.4\,\text{mm}$, $W_{s2} = 0.5\,\text{mm}$, $W_{b1} = 1.4\,\text{mm}$, $W_{b2} = 2\,\text{mm}$, $W_{g1} = 0.4\,\text{mm}$, $L_{g1} = 4.8\,\text{mm}$, and $W_{t1} = 0.33\,\text{mm}$.

3. SIMULATION AND MEASUREMENT RESULTS

The simulations for dual-mode DMDSRR are achieved with IE3D [24]. The Roger-3003 substrate with dielectric constant $\varepsilon_r = 3.0$, loss tangent $\delta = 0.0013$ and thickness $h = 1.57\,\text{mm}$ is used. For the $50\,\Omega$ line, the width is 2.8 mm, length is 16.70 mm, effective dielectric constant $\varepsilon_{eff} = 2.48$ and guided wavelength $\lambda g = 73$ mm, 5 mm and 37 mm for the frequencies $f_0 = 2.45$ GHz, 3.50 GHz and 5.20 GHz respectively.

Since the central frequencies of the responses are decided by the square loop dimensions, and the fractional BW are mainly related to the size of perturbation and the width of SIR, the variations of the parameters are investigated. The size of perturbation increases, the fractional BW in the first band increases slightly, and $P_1 = 3.3 \times 3.3\,\text{mm}^2$ is chosen at first. Then, the width of SIR decreases, the fractional BW in the second band increases slightly, and $g_1 = 1.17$ is determined. Consequently, tri-band adjustment related to perimeter ratio, tuning is needed. The perimeter ratio can be represented with the side-length ratio ($t = L_1/L_2$). If tuning in the range of $1.30 \leq t \leq 1.33$, and tri-band response is obtained.

3.1. Frequency Responses

The proposed tri-band BPF is simulated and measured with S_{21} and S_{11} frequency responses in Fig. 2. Clearly, both the simulated and measured results have good agreement. The dual-mode behaviors are presented in each band. All the tri-band responses are listed in Table 1. The lower insertion loss and higher out-of-band rejection level and wider band of the responses are obtained and it is suitable for tri-band applications. Calculation by (1) to (5), the tolerances (less than 10%) related to the measurements are also listed. The resonated frequencies shift down slightly due to the perturbation included environmental effects (temperature and interference possible).

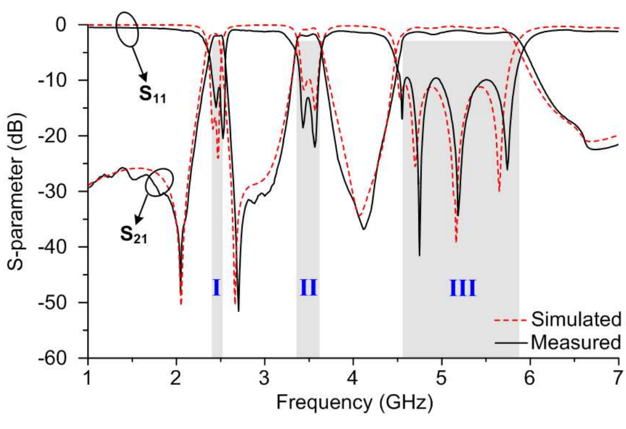

Figure 2. Frequency responses of tri-band.

Table 1. Results of tri-band responses.

Tri-band	Band-I	Band-II	Band-III
Frequency (GHz)	2.48	349	4.97
-3 dB BW (MHz)	130	240	1820
Fractional BW (%)	5.2	6.9	36.6
Maximum insertion loss (dB)	188	165	0.93
Resonances (GHz)	2.45/2.51	3.43/3.55	4.55/4.76/5.19/5.76
Transmission zero level (dB)	$-48.3/-51.7$	$-51.7/-36.9$	$-36.9/-22.6$
Calculation (GHz)	2.36	3.41	5.39
Tolerance (%)	4.8	2.3	8.5

3.2. Surface Current Distributions

Figure 3 presents the surface current distribution of tri-band DMDSRR with even and odd-modes. At the resonated frequencies in band I and II, in left column, the outer and inner rings exhibit the identical surface current distributions according to TM_{110} configuration with two more coupled magnitudes (red color) and two less coupled magnitudes (blue color) individually. Each band involves the even and odd-modes. Among the even-mode, the perturbation effects occur and the resonated frequency shifts down slightly.

In middle column, four more coupled magnitudes (red color) and four less coupled magnitudes (blue color) correspond to TM_{210} configurations are observed. The four resonated frequencies are presented in band III. Similarly, dual-mode and perturbation effects are viewed. In right column, four transmission zeroes are presented less coupled magnitudes (blue color) less coupled magnitudes (blue color) in output port. Fig. 4 presents the photograph of the proposed tri-band filters.

3.3. Comparison

When compared with the SLR filters at the same design frequency of WLAN and WiMAX system [14, 18], the performance of three filters are listed in Table 2. All filters cover the required bandwidths for WLAN band (2.4–2.48 GHz and 5.15–5.35 GHz) and WiMAX (3.4–3.6 GHz) applications. The proposed filter in this paper can significantly expend the 5.2 GHz response up to 5.8 GHz (Fractional BW = 36.6%). It covers the complete WLAN band (2.4–2.48 GHz,

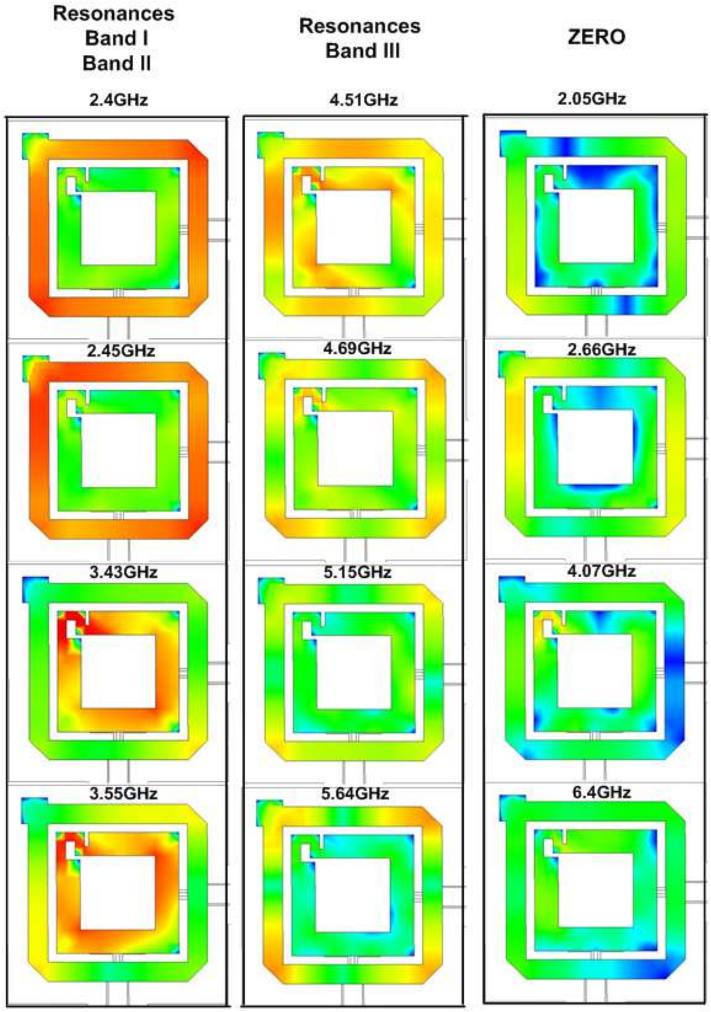

Figure 3. Surface current distribution of tri-band DMDSRR.

5.15–5.35 GHz, and 5.725–5.825 GHz). The frequency response and bandwidth in the third band are improved in the proposed filter. The return loss with in the passband is better than 20 dB and the maximum insertion losses are 1.88, 165, and 0.93 dB in the proposed filter. The maximum attenuation between the first and second passbands is 51.7 dB. The compact size is $28 \times 28 \times 1.57\,\text{mm}^3$ which is smaller the work of [18].

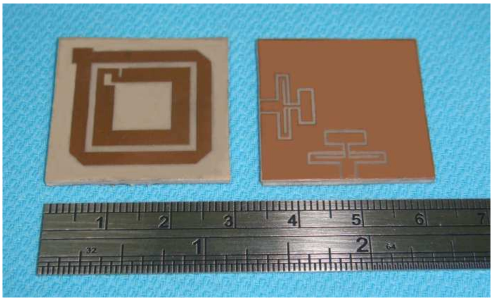

Figure 4. Photography of the proposed tri-band filters.

Table 2. Three tri-band filters for comparison.

Tri-band filters	Short/open SLR [11]	SLR and DGS [15]	This proposed DMDSLR
Resonance frequency (GHz)	2.4, 3.5 and 5.2	2.44, 3.53, and 5.26	2.44, 3.5, 5.2, and 5.8
-3 dB BW (MHz)	180, 410, and 210	300, 22, and 170	130, 24, and 1820
Fractional BW (%)	7.5, 11.7, and 4.03	12.3, 6.2, and 3.3	5.2, 6.9, and 36.6
Maximum insertion loss (dB)	1.4, 1.1, and 1.7	0.9, 1.7, and 2.1	1.88, 1.65, and 0.93
Attenuation (dB)	50, 43, 46, and 35	32, 14, 18, and 27	48.3, 51.7, 36.9, and 22.6
Size (mm^3)	$17.1 \times 17.4 \times 0.8$	$32 \times 39.5 \times 2.7$	$28 \times 28 \times 1.57$

3.4. Design Procedure

For accurate design, the effective procedure is described as follows:

Step 1. Determine the center frequency f_1, f_2 and $(f_{3a} + f_{3b})/2$ of each band.

Step 2. Select the substrate with dielectric constant, loss tangent and thickness.

Step 3. Calculate the larger side-length (L_1) and the smaller side-length (L_2) of DMDSLR by (1)–(4).

Step 4. Tune the ring perimeters to control the center frequencies by (5).

Step 5. Adjust the SIR size and meander-line width of perturbation.

Step 6. Check if perturbation could satisfy the factional bandwidth BW.

Step 7. Modify the I/O twin-T couplings structure.

Step 8. Carry out the tri-band filter.

4. CONCLUSIONS

The CPW-fed DMDSRR and the resonant frequency equations for tri-band BPF propose a viable alternative to current multi-band filter design techniques. Based on the inherent high-Q characteristics of the ring resonators, it is found that the CPW-fed DMDSRR filter can successfully present good tri-band pass-band performance, high stop-band rejection and deep transmission zeros between pass-bands. The resonant frequency equations and the design procedure are available and useful for simply designing tri-band BPF. Tuning the perimeter ratios of the rings provides four controllable resonant frequencies. Transmission zeros can be obtained by tuning the slits in the branch of the twin-T CPW.

The proposed filter has three good response bandwidths (S_{11} better than 10 dB) of 160 MHz (about 6.3% centered at 2.44 GHz), 250 MHz (about 7.3% centered at 3.50 GHz) and 1400 MHz (about 26.8% centered at 5.18 GHz), which make it easily cover the required bandwidths for WLAN band (2.4–2.48 GHz, 5.15–5.35 GHz, and 5.725–5.825 GHz) and WiMAX (3.4–3.6 GHz) applications.

REFERENCES

1. Zhang, X. Y. and Q. Xue, "Novel dual-mode dual-band filters using coplanar-waveguide-fed ring resonators," *IEEE Trans. Microwave Theory Tech.*, Vol. 55, No. 10, 2183–2190, Oct. 2007.
2. Zhang, L., Z. Y. Yu, and S. G. Mo, "Dual-mode dual-band bandpass filter using an open-loop resonator," *Journal of Electromagnetic Waves and Applications*, Vol. 23, No. 11–12, 1603–1609, 2009.
3. Chiou, Y.-C., P.-S. Yang, J.-T. Kuo, and C.-Y. Wu, "Transmission zero design graph for dual-mode dual-band filter with periodic stepped-impedance ring resonator," *Progress In Electromagnetics Research,* Vol. 108, 23–36, 2010.

4. Guo, L., Z.-Y. Yu, and L. Zhang, "Design of a dual-mode dual-band filter using stepped impedance resonators," *Progress In Electromagnetics Research Letters*, Vol. 14, 147–154, 2010.
5. Zhao, H. and T. J. Cui, "Novel triple-mode resonators using split-ring resonator," *Microwave Opt. Technol Lett.*, Vol. 49, No. 12, 2918–2922, May 2007.
6. Mokhtaari, M., J. Bomemana, K. Rambabu, and S. Amari, "Coupling matrix design of dual and triple passband filters," *IEEE Trans. Microwave Theory Tech.*, Vol. 54, No. 11, 3940–3945, Nov. 2006.
7. Lee, J. and K. Sarabandi, "Design of triple-passband microwave filters using frequency transformations," *IEEE Trans. Microwave Theory Tech.*, Vol. 56, No. 1, 187–193, Jan. 2008.
8. Chen, F. C., Q. X. Chu, and Z. H. Tu, "Tri-band bandpass filter using stub loaded resonators," *Electronics Letters*, Vol. 44, No. 12, 747–749, Jun. 2008.
9. Chen, C. F., T. Y. Huang, and R. B. Wu, "Design of dual- and triple-passband filters using alternately cascaded multiband resonators," *IEEE Trans. Microwave Theory Tech.*, Vol. 54, No. 9, 3550–3558, Sep. 2006.
10. Lee, C. H., C. I. G. Hsu, and H. K. Jhuang, "Design of a new tri-band microstrip BPF using combined quarter-wavelength SIRs," *IEEE Microw. Wireless Compon. Lett.*, Vol. 16, No. 11, 594–596, Nov. 2006.
11. Chu, Q. X. and X. M. Lin, "Advanced triple-band bandpass filter using tri-section SIR," *Electronics Lett.*, Vol. 44, No. 4, 295–296, Feb. 2008.
12. Hsu, C. I. G., C. H. Lee, and Y. H. Hsieh, "Tri-band bandpass filter with sharp passband skirts designed using tri-section SIRs," *IEEE Trans. Microwave Theory Tech.*, Vol. 18, No. 1, 19–21, Jan. 2008.
13. Chen, F. C. and Q. X. Chu, "Design of compact tri-band bandpass filters using assembled resonators," *IEEE Trans. Microwave Theory Tech.*, Vol. 57, No. 1, 165–171, Jan. 2009.
14. Chu, Q. X., F. C. Chen, Z. Tu, and H. Wang, "A novel crossed resonator and its applications to bandpass filters," *IEEE Trans. Microwave Theory Tech.*, Vol. 57, No. 7, 1753–1759, Jul. 2009.
15. Chen, B. J., T. M. Shen, and R. B. Wu, "Design of tri-band filters with improved band allocation," *IEEE Trans. Microwave Theory Tech.*, Vol. 57, No. 7, 1790–1797, Jul. 2009.
16. Zhang, X. Y., Q. Xue, and B. J. Hu, "Planar tri-band bandpass

filter with compact size," *IEEE Microw. Wireless Compon. Lett.*, Vol. 20, No. 5, 262–264, May 2010.

17. Ren, L. Y., "Tri-band bandpass filters based on dual-plane microstrip/dgs slot structure," *IEEE Microw. Wireless Compon. Lett.*, Vol. 20, No. 8, 429–431, Aug. 2010.
18. Lai, X., C. H. Liang, H. Di, and B. Wu, "Design of tri-band filter based on stub loaded resonator and DGS resonator," *IEEE Microw. Wireless Compon. Lett.*, Vol. 20, No. 5, 265–267, May 2010.
19. Lin, X. M., "Design of compact tri-band bandpass filter using $\lambda/4$ and stub-loaded resonators," *Journal of Electromagnetic Waves and Applications*, Vol. 24, No. 14–15, 2029–2035, 2010.
20. Hsu, C. I. G., C. H. Lee, and H. K. Jhuang, "Design of a novel quad-band microstrip BPF using quarter-wavelength stepped-impedance resonators," *Microw. J.*, Vol. 50, No. 2, 102–112, Feb. 2007.
21. Liu, J. C., J. W. Wang, B. H. Zeng, and D. C. Chang, "CPW-fed dual-mode double-square-ring resonators for quad-band filters," *IEEE Microw. Wireless Compon. Lett.*, Vol. 20, No. 3, 142–144, Mar. 2010.
22. Weng, R. M. and P. Y. Hsiao, "Double-layered quad-band bandpass filter for multi-band wireless systems," *Journal of Electromagnetic Waves and Applications*, Vol. 23, No. 16, 2153–2161, 2009.
23. Chang, K. and L. H. Hsieh, *Microwave Ring Circuits and Related Structures*, John Wiley & Sons, Inc., New Jersey, 2004.
24. Zeland Software Inc., IE3D version 10.0, Jan. 2005.